33rd Annual International Conference of the IEEE EMBS
Boston, Massachusetts USA, August 30 - September 3, 2011

A Comparison of Tripolar Concentric Ring Electrode and Spline Laplacians on a Four-layer Concentric Spherical Model

Xiang Liu, Student Member, IEEE, Oleksandr Makeyev, Member, IEEE and Walter Besio, Senior Member, IEEE

Abstract— **We have simulated a four-layer concentric spherical head model. We calculated the spline and tripolar Laplacian estimates and compared them to the analytical Laplacian on the spherical surface. In the simulations we used five different dipole groups and two electrode configurations. The comparison shows that the tripolar Laplacian has higher correlation coefficient to the analytical Laplacian in the electrode configurations tested (19, standard 10/20 locations and 64 electrodes).**

I. INTRODUCTION

In the last 20 years, the Brain Computer Interface (BCI) has been explored as a valuable communication channel for people who are suffering from severe motor disabilities. As a communication system that "does not depend on the brain's normal output pathways of peripheral nerves and muscles" [1], a BCI provides persons who cannot use their muscles but are cognitively intact with an alternative for communication and control.

There are primarily three types of electroencephalography (EEG) based BCIs: 1) intracortical EEG based, with electrodes placed in the brain, and 2) electrocorticogram (ECoG) based, with electrodes placed on the brain, and 3) conventional EEG based, with electrodes on the scalp (noninvasive). Among these tpyes of BCIs, noninvasive EEG based BCIs have obvious clinical benefits, but they suffer from poor spatial resolution and low signal-to-noise ratio (SNR) due to the blurring effects [2].

Cortical sources, which are at the surface of the brain, are where the imagined signals originate from for BCI. Therefore, we need to apply a high-pass spatial filter to attenuate deeper sources. Laplacian filtering has been proven to be a high-pass filter for cortical imaging [3], [4], [5]. And the surface Laplacian has been proven to produce an image proportional to the cortical potentials and enhances the high spatial frequency components of the brain activity close to the electrode [6].

To obtain the Laplacian, the most common way is to record conventional EEG and then perform digital signal processing to calculate the Laplacian from the surface potentials. Some form of interpolation is employed to create a dense sampling of the potentials and then calculate the Laplacian on the interpolated potentials. Such techniques include: a) spline Laplacian algorithm [7], b) the ellipsoidal spline Laplacian algorithm [8], c) realistic Laplacian estimation techniques [6], [9], and d) realistic geometry Laplacian algorithms [10]. Babiloni et al. demonstrated that surface Laplacian transformation of EEG signals can improve the recognition scores of imagined motor activity [11]. The surface Laplacian was also shown to give good results for focused brain activity [12], which is the case with the mental tasks that are typically used for BCIs. All the above methods for calculating the Laplacian depend on potentials recorded with disc electrodes which are prone to external and local artifacts.

Instead of employing digital signal processing methods, we are taking a new path-transforming the electrode configuration. The unique electrode configuration measures the Laplacian potential directly. This is done with the tripolar concentric ring electrode (TCRE) Fig. 1 [13]. We have shown that TCRE provided approximately four times improvement in the signal-to-noise ratio, three times improvement in spatial resolution, and twelve times improvement in mutual information compared to disc electrode signals [14]. We also found a sixteen percent improvement on single event imagined movements detection over disc signals [15]. We would now like to determine what the best spatial sampling rate and size of electrodes would be appropriate for a TCRE-based BCI. Towards this end we conducted the current work. In this paper we present the results of a comparison of the analytical, spline, and tripolar Laplacians on the surface of a 4-layer spherical model for two different spatial sampling rates.

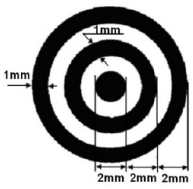

Fig. 1. Tripolar concentric ring electrode

II. METHODS

A. Four Layer Concentric Inhomogeneous Spherical Head Model

This model is introduced by B. Cuffin and D. Cohen in 1979 [16]. The four layers represent brain, cerebrospinal fluid

This work was supported by a grant from the National Science Foundation award number 0933596. We would like to thank Liling Wang for help with graphics.

Xiang Liu, Oleksandr Makeyev and Walter Besio are with the Department of Electrical, Computer, and Biomedical Engineering, University of Rhode Island, Kingston, RI, USA, 401-874-9208. liu@ele.uri.edu, omakeyev@ele.uri.edu, besio@ele.uri.edu.

and skull. The radii of the layers are: $R = 8.8cm$, $dR = 8.5cm$, $cR = 8.1cm$ and $bR = 7.9cm$; the conductivities of the layers are: $\sigma_1 = 3.3 \times 10^{-3}$, $\sigma_2 = 10.0 \times 10^{-3}$, $\sigma_3 = 4.2 \times 10^{-5}$ and $\sigma_4 = 3.3 \times 10^{-3}$ S/cm, from inside to outside respectively.

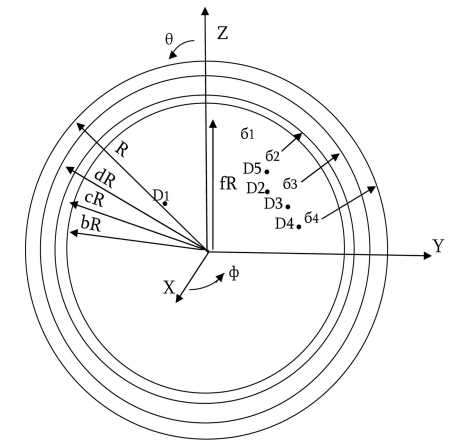

Fig. 2. Four-layer concentric spherical head model, D1 to D5 indicate the locations of dipoles employed later in the paper for testing purpose

B. Analytical Potential and Surface Laplacian

The analytical potential due to a dipole source for the 4-layer concentric inhomogeneous sphere model is given by Cuffin and Cohen[16]. Then the analytical surface Laplacian is represented by:

$$\Delta_{surf}V_x = \frac{P_x cos\phi}{4\pi\sigma_4 R^2}\sum_{n=1}^{\infty}\frac{1}{n\Gamma}\times\{(2n+1)^4 f^{n-1}(cd)^{2n+1} \times [-\frac{P_n^1(cos\theta)}{R^2 sin^2\theta} + \Delta_{surf}P_n^1(cos\theta)]\}, \tag{1}$$

$$\Delta_{surf}V_y = \frac{P_y sin\phi}{4\pi\sigma_4 R^2}\sum_{n=1}^{\infty}\frac{1}{n\Gamma}\times\{(2n+1)^4 f^{n-1}(cd)^{2n+1} \times [-\frac{P_n^1(cos\theta)}{R^2 sin^2\theta} + \Delta_{surf}P_n^1(cos\theta)]\}, \tag{2}$$

$$\Delta_{surf}V_z = \frac{P_z}{4\pi\sigma_4 R^2}\sum_{n=1}^{\infty}\frac{1}{\Gamma}\times\{(2n+1)^4 f^{n-1}(cd)^{2n+1} \times \Delta_{surf}P_n^1(cos\theta)\}, \tag{3}$$

where

$$\Delta_{surf}P_n^1(cos\theta) = \frac{1}{R^2 sin^3\theta}\{P_n(cos\theta)[n(n+1)^2 cos\theta \times sin^2\theta - (n+1)cos\theta] + P_{n+1}(cos\theta) \times [(n+1) - n(n+1)sin^2\theta]\}, \tag{4}$$

and[17],

$$\Delta_{surf}P_n(cos\theta) = -\frac{n(n+1)}{R^2}P_n(cos\theta). \tag{5}$$

C. Spline Potential and Surface Laplacian

The potential distribution on the spherical surface is estimated by the spline interpolation [9]:

$$V(x,y,z) = \sum_{i=1}^{N} t_i H_{m-1}(x-x_i, y-y_i, z-z_i) + R_{m-1}(x,y,z), \tag{6}$$

where m is the spline order, N is the number of samples, (x_i, y_i, z_i) are the location of the i^{th} sample. And

$$H_{m-1}(x-x_i, y-y_i, z-z_i) = ((x-x_i)^2 + (y-y_i)^2 + (z-z_i)^2)^{(2m-3)/2}, \tag{7}$$

$$R_{m-1}(x,y,z) = \sum_{d=0}^{m-1}\sum_{k=0}^{d}\sum_{g=0}^{k} r_{dkg}x^{d-k}y^{k-g}z^g, \tag{8}$$

t_i and r_{dkg} are obtained from:

$$\begin{aligned}&(H+\lambda I)\cdot T + F\cdot R = V\\ &F^t\cdot T = 0,\end{aligned} \tag{9}$$

where

$$\begin{aligned}H &= (h_{ij}) = H_{m-1}(x_i-x_j, y_i-y_j, z_i-z_j)\\ R^t &= (r_{00} \quad r_{01} \quad r_{11} \quad \cdots \quad r_{m-1m-1})\\ T^t &= (t_1 \quad t_2 \quad t_3 \quad \cdots \quad t_n)\\ V^t &= (v_1 \quad v_2 \quad v_3 \quad \cdots \quad v_n),\end{aligned} \tag{10}$$

$$F = \begin{bmatrix}1 & x_1 & y_1 & z_1 & x_1^2 & \cdots & y_1z_1 & z_1^2\\ \cdot & \cdot & \cdot & \cdot & \cdot & \cdot & \cdot & \cdot\\ \cdot & \cdot & \cdot & \cdot & \cdot & \cdot & \cdot & \cdot\\ \cdot & \cdot & \cdot & \cdot & \cdot & \cdot & \cdot & \cdot\\ 1 & x_N & y_N & z_N & x_N^2 & \cdots & y_Nz_N & z_N^2\end{bmatrix} \tag{11}$$

Parameter λ in Eq.(9) is adjustable to achieve the best estimation of the potential on the sphere surface [18], [19], [6].

By applying the surface Laplacian operator to Eq. (6), and employing the spherical coordinates system for the calculation, the Laplacian is given by:

$$\Delta_{surf}V(x,y,z) = \sum_{i=1}^{N} t_i(\frac{cos\theta}{R^2 sin\theta}\frac{\partial H_{m-1}}{\partial\theta} + \frac{1}{R^2}\frac{\partial^2 H_{m-1}}{\partial\theta^2} + \frac{1}{R^2 sin^2\theta}\frac{\partial^2 H_{m-1}}{\partial\phi^2}) + (\frac{cos\theta}{R^2 sin\theta}\frac{\partial R_{m-1}}{\partial\theta} + \frac{1}{R^2}\frac{\partial^2 R_{m-1}}{\partial\theta^2} + \frac{1}{R^2 sin^2\theta}\frac{\partial^2 R_{m-1}}{\partial\phi^2}), \tag{12}$$

where

$$\frac{\partial H_{m-1}}{\partial\theta} = -(2m-3)R(x_i cos\theta cos\phi + y_i cos\theta sin\phi - z_i sin\theta)(R^2 + x_i^2 + y_i^2 + z_i^2 - 2R(x_i sin\theta \times cos\phi + y_i sin\theta sin\phi + z_i cos\theta))^{(2m-5)/2}, \tag{13}$$

$$\frac{\partial^2 H_{m-1}}{\partial\theta^2} = (2m-3)R(x_i sin\theta cos\phi + y_i sin\theta sin\phi + z_i cos\theta)(R^2 + x_i^2 + y_i^2 + z_i^2 - 2R(x_i sin\theta \times cos\phi + y_i sin\theta sin\phi + z_i cos\theta))^{(2m-5)/2} + (2m-3)(2m-5)t_i R^2(x_i cos\theta cos\phi + y_i cos\theta sin\phi - z_i sin\theta)^2(R^2 + x_i^2 + y_i^2 + z_i^2 - 2R(x_i sin\theta cos\phi + y_i sin\theta sin\phi + z_i cos\theta))^{(2m-7)/2}, \quad (14)$$

$$\frac{\partial^2 H_{m-1}}{\partial\phi^2} = (2m-3)R(x_i sin\theta cos\phi + y_i sin\theta sin\phi)(R^2 + x_i^2 + y_i^2 + z_i^2 - 2R(x_i sin\theta cos\phi + y_i sin\theta sin\phi + z_i cos\theta))^{(2m-5)/2} + (2m-3)(2m-5)t_i R(x_i sin\theta sin\phi - y_i sin\theta \times cos\phi)^2(R^2 + x_i^2 + y_i^2 + z_i^2 - 2R(x_i sin\theta \times cos\phi + y_i sin\theta sin\phi + z_i cos\theta)^{(2m-7)/2}, \quad (15)$$

$$\frac{\partial R_{m-1}}{\partial\theta} = r_{dkg} R^d((d-g)sin^{d-g-1}\theta cos^{g+1}\theta - g sin^{d-g+1}\theta cos^{g-1}\theta) sin^{k-g}\phi cos^{d-k}\phi, \quad (16)$$

$$\frac{\partial^2 R_{m-1}}{\partial\theta^2} = r_{dkg} R^d sin^{k-g}\phi cos^{d-k}\phi[(d-g)\times (d-g-1)sin^{d-g-2}\theta cos^{g+2}\theta - (d-g+1)g sin^{d-g}\theta cos^g\theta - (d-g) \times (g+1)sin^{d-g}\theta cos^g\theta + (g-1)g sin^{d-g+2}\theta cos^{g-2}\theta], \quad (17)$$

$$\frac{\partial^2 R_{m-1}}{\partial\phi^2} = r_{dkg} R^d sin^{d-g}\theta cos^g\theta((k-g)\times (k-g-1)sin^{k-g-2}\phi cos^{d-k+2}\phi - (k-g)(d-k+1)sin^{k-g}\phi cos^{d-k}\phi) - (d-k)(k-g+1)sin^{k-g}\phi cos^{d-k}\phi + (d-k)(d-k+1)sin^{k-g+2}\phi cos^{d-k-2}\phi, \quad (18)$$

where θ is the polar angle, ϕ is the azimuthal angle of the spherical coordinate system.

D. Tripolar Laplacian

The tripolar Laplacian was introduced previously [13]. Besio et al. showed that the tripolar Laplacian is given by the combination of the potentials from the three elements of the TCRE:

$$Laplacian = \frac{16(V_m - V_d) - (V_o - V_d)}{3R_m^2}, \quad (19)$$

where V_d is the potential of the central disc, V_m is the potential of the middle ring, V_o is the potential of the outer ring and R_m is the radius of the middle ring.

TABLE I

POSITIONS AND MOMENTS OF THE 5 DIPOLES

Dipole	Position(cm)			Moment		
	x	y	z	mx	my	mz
1	+4.0	−3.0	+3.5	+4.0	−2.0	+3.0
2	+3.5	+3.0	+4.0	+3.0	+5.0	+1.0
3	−2.5	+4.5	+3.0	+2.0	−4.0	+6.0
4	−3.0	+5.0	+2.0	+3.0	+2.0	+0.0
5	+1.0	+3.0	+5.0	−5.0	+1.0	−3.0

E. Simulation Protocol

In order to simulate the potentials on the rings of the TCRE electrode, we calculated the potentials at "sampling points" uniformly distributed on the rings and the central disc of the TCRE. The potential for a corresponding ring was the average of potentials at these "sampling points". To determine the number of "sampling points" necessary for stable calculations we examined the effect of the "sampling points" density on the averaged potential. The basic concept was that the higher the density of uniformly distributed "sampling points", the closer the averaged potential is to the real potential. In our initial analysis we incrementally increased the density of "sampling points" on the TCRE and compared the averaged potential. When the difference in potential due to adding more points was less than 0.1 percent then we considered that the density of "sampling points" was accurate enough for our simulation.

To simulate the cortical activities of the brain, five groups of dipoles in the brain sphere were employed in the simulation. Each group contained one or two dipoles randomly selected from five dipoles (Table I). Two electrode montages, 19 electrodes, from the 10-20 system, or 64 electrodes selected from the 10-5 system [20], were employed to study the effect of the number of recording electrodes to the Laplacian. The potentials were interpolated using the spline routine of Eq. (6) with the Laplacian calculated with Eq. (12). The tripolar Laplacian was also calculated at the electrodes locations, and both were evaluated in terms of correlation coefficient (CC) with respect to the analytical Laplacian.

III. RESULTS

Potentials were calculated for different dipole configurations. From the two electrode configurations, CC values between the spline Laplacian and analytical Laplacian, as well as between tripolar Laplacian and analytical Laplacian are shown in Table II.

Table II shows that the performance of the spline Laplacian has a direct proportion with the number of recording electrodes. This is reasonable since the spline parameters should be better estimated with more recording electrodes, higher spatial sampling. Table II also indicates that the tripolar Laplacian has superior performance compared to the spline Laplacian, especially in low spatial sampling situations (with less recording electrodes). This is due to the directly obtained local Laplacian of the TCRE, which means it doesn't rely

TABLE II

CORRELATION COEFFICIENT (CC) BETWEEN THE SPLINE AND TRIPOLAR LAPLACIAN WITH RESPECT TO THE ANALYTICAL LAPLACIAN. CONFIG I: 19 ELECTRODES FROM 10-20 SYSTEM, CONFIG II: 64 ELECTRODES SELECTED FROM 10-5 SYSTEM, SL: SPLINE LAPLACIAN, TL: TRIPOLAR LAPLACIAN.

Dipoles	Config I		Config II	
	SL	TL	SL	TL
1	0.81	0.99	0.98	0.99
2	0.89	0.99	0.97	0.99
3&4	0.91	0.99	0.97	0.99
2&5	0.95	0.99	0.98	0.99
1&3	0.79	0.99	0.97	0.99

on the number of recording electrodes. We also saw that different dipole configurations did not effect the tripolar Laplacian accuracy.

IV. DISCUSSION

The tripolar Laplacian recorded from the TCRE is a local-based Laplacian[21], [22], [23], [24], which calculates the Laplacian from a limited area on the surface. While the spline Laplacian is considered a global Laplacian, where the spline Laplacian at any location depends on the potentials from all the recording electrodes. Although the spline Laplacian has been shown to have better performance than the local Laplacian [6], our simulation indicates that in low spatial sampling situations our TCRE produces better Laplacian estimates than the spline Laplacian.

V. CONCLUSION

The tripolar Laplacian produced by our TCRE has higher CC with respect to the analytical Laplacian than the spline Laplacian in low sampling situations.

REFERENCES

[1] Wolpaw J. R., McFarland D. J., and Vaughan T. M., Brain-computer interface research at the Wadsworth Center, *IEEE Trans. Rehab. Eng.*, vol. 8, no. 2, pp. 222-226, Jun. 2000.

[2] Nunez P. L., Silberstein R. B., Cadiush P. J., Wijesinghe J., Westdorp A. F., and Srinivasan R., A theoretical and experimental study of high resolution EEG based on surface Laplacians and cortical imaging, *EEG Clin. Neurophysiol.*, vol. 90, pp. 40-57, 1994.

[3] Nunez P. L., Electric Fields of the Brain: The Neurophysics of EEG, Oxford University Press, New York, 1981.

[4] Srinivasan R., Methods to Improve the Spatial Resolution of EEG, *IJBEM*, 1(1), 102-111, 1999.

[5] Kramer M., and Szeri A., Quantitative approach of the cortical surface potential from EEG and ECoG measurements, *IEEE TBME*, VOL. 51 NO. 8 1358-1365, 2004.

[6] Babiloni F., Babiloni C., Carducci F., Fattorini L., Onorati P., and Urbano A., Performances of surface laplacian estimators: a study of simulated and real scalp potential distributions, *Brain Topogr.*, vol. 8, pp.35-45, 1995.

[7] Perrin F., Bertrand O., and Pernier J., Scalp current density mapping: value and estimation from potential data, *IEEE Trans. Biomed. Eng.*, vol. BME-34, pp. 283-288, 1987.

[8] Law S. K., Nunez P. L., and Wijesinghe R. S., High resolution EEG using spline generated surface Laplacians on spherical and ellipsoidal surfaces, *IEEE Trans Biomed Eng.*, vol. 40, no. 2, pp. 145-153, Feb.1993.

[9] Babiloni F., Babiloni C., Carducci F., Spline laplacian estimate of EEG potentials over a realistic magnet resonance constructed scalp surface model, *EEG Clin. Neurophysiol.*, vol. 98, pp. 363-373, 1996.

[10] He B., Lian J., and Li G., High-resolution EEG: a new realistic geometry spline laplacian estimation technique, *Clin. Neurophysiol.*, vol.112, pp. 845-852, 2001.

[11] Babiloni F., Cincotti F., Lazzarini L., Milan J., Mourino J., Varsta M., Heikkonen J., Bianchi L., and Marciani M. G., Linear Classification of Low-Resolution EEG Patterns Produced by Imagined Hand Movements, *IEEE Transactions on Rehabilitation engineering*, Vol. 8, No. 2, 186-188, June 2000.

[12] Pfurtscheller G., and Lopes da Silva F. H. , Event-related EEG/MEG synchronization and desynchronization: Basic principles, *Clin. Neurophysiol.*,vol. 110, pp. 1842-1857, 1999.

[13] Besio W., Koka K., Aakula R., Dai W., Tri-polar Concentric Ring Electrode Development for Laplacian Electroencephalography, *IEEE Trans BME*, Vol. 53, No. 5, pp. 926-933, 2006.

[14] Koka K., Besio W., Improvement of spatial selectivity and decrease of mutual information of tri polar concentric ring electrodes. *J Neuroscience Methods.*, 2007, 165: 216-222.

[15] Besio W., Cao H. Zhou P., Application of Tripolar Concentric Electrodes and Prefeature Selection Algorithm for BrainCComputer Interface. *Neural Systems and Rehabilitation Engineering, IEEE Transactions on*, 2008, Volume 16 Issue 2: 191-194.

[16] Cuffin B. N., and D. Cohen, Comparison of the magnetoencephalogram and electroencephalogram, *Electroencephalography and Clinical Neurophysiology*, 47, 132-146, 1979.

[17] Arfken, G. B., and Weber H. J., Mathematical methods for physicists, Academic Press, 1995.

[18] Harder, R., and Desmarais, R., Interpolation using surface splines. *J. Aircraft*, 1972, 9: 189-191.

[19] Le, J., Vinod, M. and Gevins, A., Local estimate of surface Laplacian derivation on a realistically shaped scalp surface and its performance on noisy data, *Electroenceph. clin. Neurophysiol.*, 1994, 92:433-441.

[20] Oostenveld R., Praamstra P., The five percent electrode system for high-resolution EEG and ERP measurements, *Clin Neurophysiol.*,112(4):713-719, 2001.

[21] Hjorth B, An on-line transformation of EEG scalp potentials into orthogonal source derivations, *EEG. Clin. Neurophysiol.*, vol. 39, pp.526-530, 1975.

[22] McKay, D.M., On-line source density computation with a minimum of electrodes, *Electroenceph. clin. Neurophysiol.*, 1983, 56: 696-698.

[23] Thickbroom, G. W., Mastaglia, F.L., Carroll, W.M. and Davies, H.D. Source derivation: application to topographic mapping of visual evoked potentials. *Electroenceph. clin. Neurophysiol.*, 1984, 59: 279-285.

[24] Gevins, A., Dynamic functional topography of cognitive task. *Brain Topogr.*, 1989, 2: 37-56.